14
Deep-inelastic scattering from the nucleon

We proceed to a discussion of inclusive deep-inelastic electron scattering from the nucleon $N(e,e')_{DIS}$. Here both the four-momentum transfer q^2 and energy transfer $\nu = q \cdot p/m$ become very large.[1] It is through these experiments, initially carried out at the Stanford Linear Accelerator Center (SLAC), that the first dynamic evidence for a point-like substructure of hadrons was obtained [Bj69, Fr72]. The structure functions exhibit this point-like substructure through Bjorken *scaling*, which implies $F_i(q^2,\nu) \to F_i(q^2/\nu)$ as $q^2 \to \infty$ and $\nu \to \infty$ at fixed q^2/ν. To set the stage for the discussion in this section, we first review some of our general considerations on electron scattering [Qu83, Wa84] which form an essential basis for what follows. The experimental deep-inelastic results are then summarized [Fr72, Bj69, Qu83]. Finally, the quark–parton model is developed. It is through the quark–parton model that the deep-inelastic scaling was first understood [Fe69, Bj69a, Ha84, Ai89, Ma90].[2] The change of the structure functions in nuclei (EMC effect) gives direct evidence for the modification of quark properties in the nuclear medium [Au83], and this is briefly discussed.

The kinematics for electron scattering employed in this section are shown in Fig. 14.1. Here the four-momentum transfer is defined by[3]

$$\begin{aligned} q &= k_2 - k_1 = p - p' \\ q^2 &= 4\varepsilon_1\varepsilon_2 \sin^2\frac{\theta}{2} \qquad ; \text{ lab} \end{aligned} \tag{14.1}$$

[1] We revert here to the previous notation where q denotes the momentum transfer in an inclusive process.

[2] QCD then allows a calculation of the *corrections* to scaling and the evolution equations for doing this [Al77] are discussed, for example, in [Wa95].

[3] Massless electrons are again assumed throughout this discussion.

https://doi.org/10.1017/9781009290616.017 Published online by Cambridge University Press

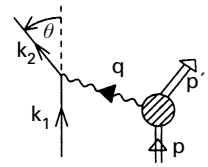

Fig. 14.1. Kinematics in electron scattering; momenta are four-vectors.

We further define

$$\begin{aligned} \nu &\equiv \frac{q\cdot p}{m} \\ &= \varepsilon_1 - \varepsilon_2 \qquad\qquad ;\ \text{lab} \\ x &\equiv \frac{q^2}{2m\nu} \end{aligned} \tag{14.2}$$

These are the energy loss in the lab frame and Bjorken scaling variable, respectively.

The S-matrix for the process in Fig. 14.1 is given by

$$S_{fi} = -\frac{(2\pi)^4}{\Omega}\delta^{(4)}(k_1 + p - k_2 - p')ee_p\bar{u}(k_2)\gamma_\mu u(k_1)\frac{1}{q^2}\langle p'|J_\mu(0)|p\rangle \tag{14.3}$$

Here $J_\mu(x)$ is the local electromagnetic current operator for the target system. With box normalization,[4] momentum conservation is actually expressed through the relation

$$\frac{(2\pi)^3}{\Omega}\delta^{(3)}(\mathbf{k}_1 + \mathbf{p} - \mathbf{k}_2 - \mathbf{p}') \doteq \delta_{\mathbf{k}_1+\mathbf{p},\mathbf{k}_2+\mathbf{p}'} \tag{14.4}$$

The incident flux in any frame where $\mathbf{k}_1 || \mathbf{p}$ is given by

$$I_0 = \frac{1}{\Omega}\frac{\sqrt{(k_1\cdot p)^2}}{\varepsilon_1 E_p} \tag{14.5}$$

Then for a one-body nuclear final state

$$\begin{aligned} S_{fi} &\equiv -2\pi i\,\delta(\varepsilon_1 + E_p - \varepsilon_2 - E_{p'})\delta_{\mathbf{k}_1+\mathbf{p},\mathbf{k}_2+\mathbf{p}'}\bar{T}_{fi} \\ d\sigma_{fi} &= 2\pi|\bar{T}_{fi}|^2\delta(W_f - W_i)\frac{\Omega d^3k_2}{(2\pi)^3}\left[\frac{1}{\Omega}\frac{\sqrt{(k_1\cdot p)^2}}{\varepsilon_1 E_p}\right]^{-1} \end{aligned} \tag{14.6}$$

Here $W_f = \varepsilon_2 + E_{p'}$ and $W_i = \varepsilon_1 + E_p$ are the total final and initial energies, respectively. It follows that the differential cross section in any

[4] That is, periodic boundary conditions in a big box of volume Ω.

https://doi.org/10.1017/9781009290616.017 Published online by Cambridge University Press

frame where $\mathbf{k}_1||\mathbf{p}$ is given in Lorentz invariant form by

$$d\sigma = \frac{4\alpha^2}{q^4}\frac{d^3k_2}{2\varepsilon_2}\frac{1}{\sqrt{(k_1\cdot p)^2}}\eta_{\mu\nu}W_{\mu\nu} \tag{14.7}$$

In this expression the lepton and hadron tensors for unpolarized electrons and targets, generalized to include arbitrary nuclear final states, are defined by

$$\begin{aligned}\eta_{\mu\nu} &= -2\varepsilon_1\varepsilon_2\frac{1}{2}\sum_{s_1}\sum_{s_2}\bar{u}(k_1)\gamma_\nu u(k_2)\bar{u}(k_2)\gamma_\mu u(k_1) \qquad (14.8)\\ W_{\mu\nu} &= (2\pi)^3\Omega\overline{\sum_i}\sum_f\delta^{(4)}(q+p'-p)\langle p|J_\nu(0)|p'\rangle\langle p'|J_\mu(0)|p\rangle E_p\end{aligned}$$

The lepton tensor can be evaluated directly (recall the mass of the electron is neglected)

$$\begin{aligned}\eta_{\mu\nu} &= -2\varepsilon_1\varepsilon_2\frac{1}{2}\text{trace}\frac{(-ik_{1\lambda}\gamma_\lambda)}{2\varepsilon_1}\gamma_\nu\frac{(-ik_{2\rho}\gamma_\rho)}{2\varepsilon_2}\gamma_\mu\\ &= k_{1\mu}k_{2\nu}+k_{1\nu}k_{2\mu}-(k_1\cdot k_2)\delta_{\mu\nu} \qquad (14.9)\end{aligned}$$

It follows from the definition in Eq. (14.8) that the lepton current is conserved

$$q_\mu\eta_{\mu\nu} = \eta_{\mu\nu}q_\nu = 0 \tag{14.10}$$

The hadron tensor depends on just the two four-vectors (q,p) and is also conserved; its general form is

$$\begin{aligned}W_{\mu\nu} &= W_1(q^2,q\cdot p)\left(\delta_{\mu\nu}-\frac{q_\mu q_\nu}{q^2}\right)\\ &\quad +W_2(q^2,q\cdot p)\frac{1}{m^2}\left(p_\mu-\frac{q\cdot p}{q^2}q_\mu\right)\left(p_\nu-\frac{q\cdot p}{q^2}q_\nu\right) \qquad (14.11)\end{aligned}$$

With this background, let us proceed to further analyze the hadronic response tensor. The Heisenberg equations of motion for the target are as follows:

$$\hat{O}(x) = e^{-i\hat{P}\cdot x}\hat{O}(0)e^{i\hat{P}\cdot x} \tag{14.12}$$

They can be used to exhibit the space-time dependence of a matrix element taken between eigenstates of four-momentum

$$\begin{aligned}W_{\mu\nu} &= \frac{1}{2\pi}(\Omega E)\overline{\sum_i}\sum_f\int e^{iq\cdot z}d^4z\langle p|J_\nu(z)|p'\rangle\langle p'|J_\mu(0)|p\rangle\\ &= \frac{1}{2\pi}(\Omega E)\overline{\sum_i}\int e^{iq\cdot z}d^4z\langle p|J_\nu(z)J_\mu(0)|p\rangle \qquad (14.13)\end{aligned}$$

https://doi.org/10.1017/9781009290616.017 Published online by Cambridge University Press

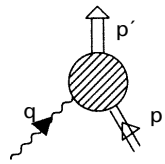

Fig. 14.2. Kinematics for crossed term.

Completeness of the final set of hadronic states has been used to obtain the second line. Consider the matrix elements of the operators in the opposite order

$$\int e^{iq\cdot z} d^4z \langle p|J_\mu(0)J_\nu(z)|p\rangle \propto \sum_f (2\pi)^4 \delta^{(4)}(p+q-p')\langle p|J_\mu(0)|p'\rangle\langle p'|J_\nu(0)|p\rangle \tag{14.14}$$

Here the kinematics are illustrated in Fig. 14.2

$$\begin{aligned} p+q &= p' \\ q_0 &= \varepsilon_2 - \varepsilon_1 < 0 \end{aligned} \tag{14.15}$$

One cannot reach a physical state under these kinematic conditions since the nucleon is *stable*; thus the expression in Eq. (14.14) vanishes. One can subtract this vanishing term in Eq. (14.13) and write $W_{\mu\nu}$ as the Fourier transform of the commutator of the current density at two displaced space-time points

$$W_{\mu\nu} = \frac{1}{2\pi}(\Omega E)\overline{\sum_i} \int e^{iq\cdot z} d^4z \langle p|[J_\nu(z), J_\mu(0)]|p\rangle \tag{14.16}$$

Introduce states with *covariant norm*[5]

$$|p) \equiv \sqrt{2E\,\Omega}\,|p\rangle \tag{14.17}$$

Equation (14.13) can then be rewritten

$$-\pi W_{\mu\nu} \equiv t_{\mu\nu} = -\frac{1}{4}\overline{\sum_i} \int e^{iq\cdot z} d^4z\, (p|[J_\nu(z), J_\mu(0)]|p) \tag{14.18}$$

This expression is evidently covariant; it forms the absorptive part of the amplitude for forward, virtual Compton scattering. Since the currents are observables, their commutator must vanish outside the light cone. Thus the only contribution to this integral comes from inside the light cone.

[5] The norm of these states is $\left(\vec{p}\,|\vec{p}\,'\right) = 2E(2\pi)^3\delta^{(3)}(\vec{p}-\vec{p}\,')$; this is Lorentz invariant.

https://doi.org/10.1017/9781009290616.017 Published online by Cambridge University Press

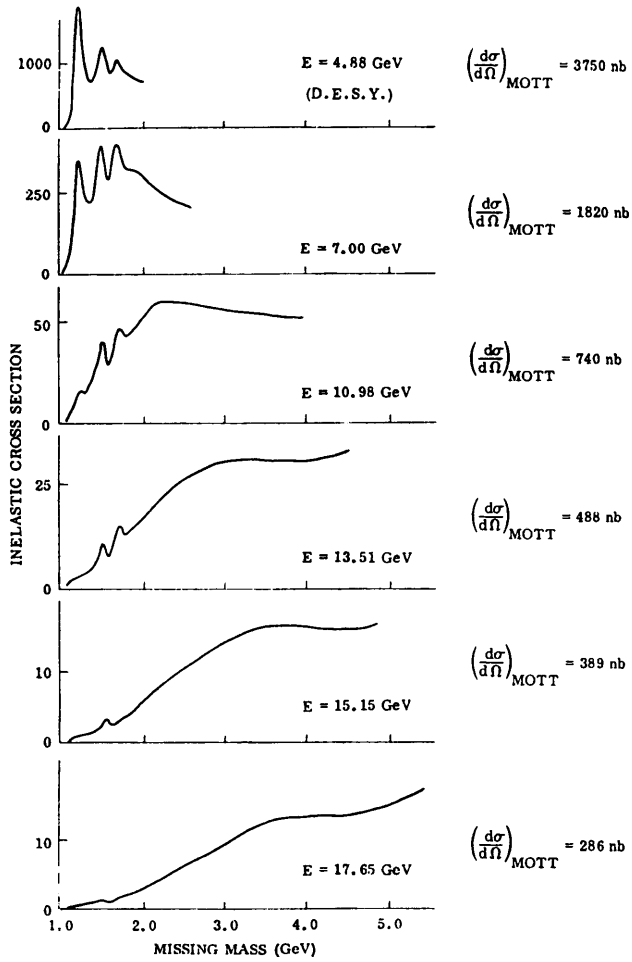

Fig. 14.3. Visual fits to spectra showing the scattering of electrons from hydrogen at $\theta = 10^{o}$ for primary energies 4.88 to 17.65 GeV. The elastic peaks have been subtracted and radiative corrections applied. The cross sections are expressed in nanobarns/GeV/steradian [Fr72].

In the Bjorken scaling limit, the dominant contribution to this integral comes, in fact, from singularities *on* the light cone (see e.g. [De73]). This observation forms the basis for a covariant, field theory evaluation of the structure functions and systematic determination of corrections. The light-cone analysis of this expression is discussed in more detail in appendix I.

A combination of Eqs. (14.7), (14.9), and (14.11) yields the general form of the laboratory cross section for the scattering of unpolarized (massless)

https://doi.org/10.1017/9781009290616.017 Published online by Cambridge University Press

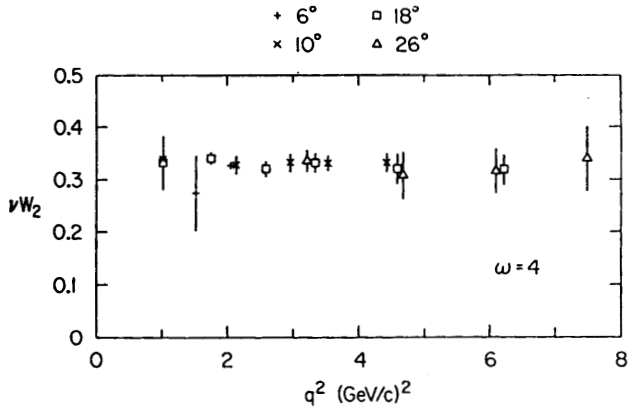

Fig. 14.4. νW_2 for the proton as a function of q^2 and total C-M energy of the proton and virtual photon $W = [-(p-q)^2]^{1/2} > 2\,\text{GeV}$ at $\omega = 1/x = 4$ [Fr72].

electrons from an unpolarized nucleon

$$\begin{aligned} \frac{d^2\sigma}{d\Omega_2 d\varepsilon_2} &= \sigma_M \frac{1}{m}\left[W_2(\nu, q^2) + 2W_1(\nu, q^2)\tan^2\frac{\theta}{2}\right] \\ \sigma_{\text{M}} &= \frac{\alpha^2\cos^2\theta/2}{4\varepsilon_1^2\sin^4\theta/2} \end{aligned} \tag{14.19}$$

Here σ_{M} is the Mott cross section.

A qualitative overview of the SLAC data on deep-inelastic electron scattering from the proton is shown in Fig. 14.3 [Fr72]. On the basis of his analysis of various sum rules, Bjorken *predicted*, before the experiments, the following behavior of the structure functions in the deep-inelastic regime [Bj69]

$$\begin{aligned} \frac{\nu}{m}W_2(\nu, q^2) &\to F_2(x) \qquad ;\ q^2 \to \infty, \quad \nu \to \infty \\ 2W_1(\nu, q^2) &\to F_1(x) \end{aligned} \tag{14.20}$$

Here the scaling variable is defined by

$$x \equiv \frac{q^2}{2m\nu} \equiv \frac{1}{\omega} \tag{14.21}$$

These relations imply that the structure functions do not depend individually on (ν, q^2) but only on their *ratio*. The scaling behavior of the SLAC data is shown in Figs. 14.4 and 14.5 [Fr72].[6] The first of these figures

[6] These authors use $W_{1,2} \equiv (1/m)W_{1,2}^{\text{text}}$ where $W_{1,2}^{\text{text}}$ are the structure functions used here.

https://doi.org/10.1017/9781009290616.017 Published online by Cambridge University Press

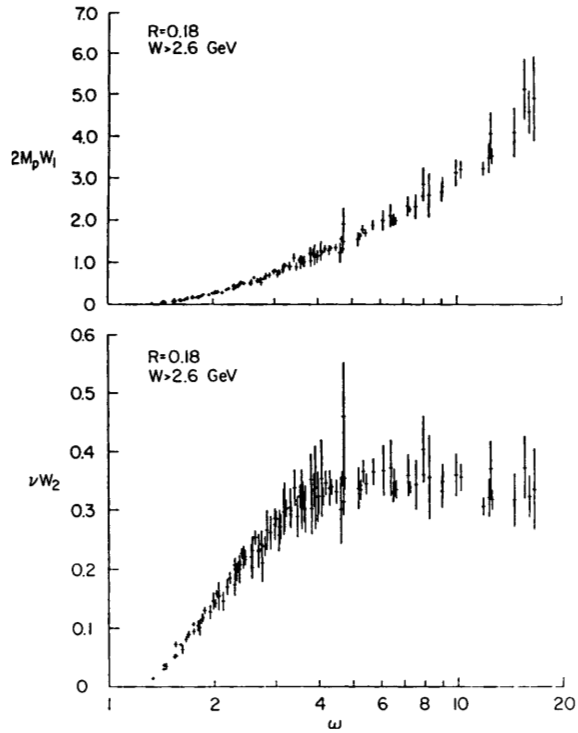

Fig. 14.5. Structure functions $2mW_1$ and νW_2 for the proton vs ω for C-M energy $W > 2.6\,\text{GeV}$ and $q^2 > 1\,(\text{GeV/c})^2$, and using R = 0.18 [Fr72].

illustrates the independence from q^2 at fixed $\omega = 1/x$; the second shows the extracted structure functions $F_{1,2}(x)$.[7]

Let us now turn to an interpretation of these experimental results. The empirical data on deep-inelastic electron scattering can be understood within the framework of the *quark–parton model* developed for that purpose by Feynman and Bjorken and Paschos [Fe69, Bj69a]. The basic concepts in the model are as follows:

- The calculation of the structure functions is Lorentz invariant. Go to the C-M frame of the proton and incident electron with $\mathbf{p} = -\mathbf{k}_1$. Now let the proton move very fast with $|\mathbf{p}| \to \infty$. This forms the *infinite-momentum frame*; it is illustrated in Fig. 14.6.
- Assume the nucleon is composed of a substructure of *partons*. The proper motion of the parton constituents of the hadron (here a proton) is slowed down by time dilation in the infinite-momentum

[7] From the SLAC data the ratio of longitudinal to transverse cross section is given by $R \equiv \sigma_l/\sigma_t = 0.18 \pm 0.10$ where $W_1/W_2 \equiv (1 + \nu^2/q^2)\sigma_t/(\sigma_t + \sigma_l)$.

https://doi.org/10.1017/9781009290616.017 Published online by Cambridge University Press

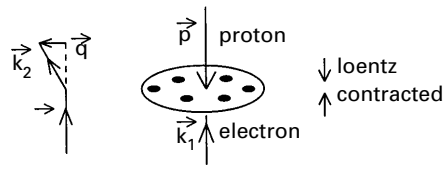

Fig. 14.6. Situation in frame where the proton is moving very rapidly with momentum $\mathbf{p} = -\mathbf{k}_1$ (the infinite-momentum frame).

frame. Thus the partons are effectively *frozen* during the scattering process. The actual interaction between the partons is then not important.

- Assume that the very-short-wavelength electrons scatter *incoherently* from the constituents. Assume further that the constituent partons have no internal electromagnetic structure and that the electrons scatter from the charged constituents as if they are *pointlike Dirac particles.*

- Assume that in the limit $q^2 \to \infty, \nu \to \infty$, the masses of the constituents can be neglected. Assume also that the transverse momentum of the parton before the collision, determined by the internal structure of the hadron and the strong-interaction dynamics, can be neglected in comparison with $\sqrt{q^2}$, the transverse momentum imparted as $|\vec{p}\,| \to \infty$.

We now know from subsequent developments, largely motivated by these deep-inelastic electron scattering experiments and the success of the quark–parton model, that the parton constituents of the hadron are actually quarks (charged) and gluons (neutral).

The scaling results can be understood within the framework of the *impulse approximation* applied to this model.[8] The calculation of the cross section is Lorentz invariant, and can be performed in any Lorentz frame, in particular in any frame where $\mathbf{p} \| \mathbf{k}_1$. Go to the infinite-momentum frame. The scattering situation is then illustrated in Fig. 14.7. In this frame the ith parton carries the incident four-momentum

$$p_{\text{inc}} \quad = \quad \eta_i \, p \tag{14.22}$$

Here η_i is the fraction of the four-momentum p of the proton carried by the ith parton. Evidently

$$0 \leq \eta_i \leq 1 \tag{14.23}$$

[8] This discussion is based on [Ha84, Ai89, Ma90, Wa95].

https://doi.org/10.1017/9781009290616.017 Published online by Cambridge University Press

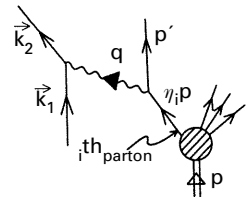

Fig. 14.7. Scattering in impulse approximation in the quark–parton model in the infinite-momentum frame.

The incident hadron is now just a collection of independent partons. The electron proceeds to scatter from one of the point-like charged partons. We do not worry here about how the parton eventually gets converted into hadrons in the final state (*hadronization*). Only the quarks are charged with charges

$$q_i \equiv Q_i e_p \tag{14.24}$$

Now

> *Let $f_i(\eta_i)d\eta_i$ be the number of quarks of type i with four-momentum between $\eta_i p$ and $(\eta_i + d\eta_i)p$.*

The total four-momentum of the proton is then evidently given by

$$\begin{aligned} p &= p_{\text{gluons}} + p_{\text{quarks}} \\ p &= \zeta_g p + \sum_{i=1}^{N} \int_0^1 (\eta_i p) f_i(\eta_i) d\eta_i \end{aligned} \tag{14.25}$$

Here ζ_g is the fraction of the total four-momentum of the proton carried by all the gluons, and $\sum_{i=1}^{N}$ is a sum over all types of quarks.

Cancellation of an overall factor of the four-momentum p from the last of Eqs. (14.25) gives

$$1 = \zeta_g + \sum_{i=1}^{N} \int_0^1 \eta_i f_i(\eta_i) d\eta_i \tag{14.26}$$

Introduce a dummy variable x; this *momentum sum rule* can then be written

$$\begin{aligned} 1 &= \zeta_g + \sum_{i=1}^{N} \zeta_i \\ \zeta_i &\equiv \int_0^1 x f_i(x) dx \end{aligned} \tag{14.27}$$

Now calculate the process in Fig. 14.7 using the analysis of inelastic electron scattering presented at the beginning of this chapter. With the

https://doi.org/10.1017/9781009290616.017 Published online by Cambridge University Press

assumption of scattering from point-like Dirac particles, the S-matrix for scattering from an isolated quark of type i is given by[9]

$$\begin{aligned} S^{(i)} &= \frac{-i(2\pi)^4 e e_p Q_i}{\Omega^2 q^2}\delta^{(4)}(p'+q-\eta_i p)\bar{u}(k_2)\gamma_\mu u(k_1)\bar{u}(p')\gamma_\mu u(\eta_i p) \\ &\equiv -\frac{(2\pi)^4 i}{\Omega}\delta^{(4)}(p'+q-\eta_i p)\bar{T}^{(i)} \end{aligned} \tag{14.28}$$

The incident flux is given by

$$I_0 = \frac{1}{\Omega}\frac{\sqrt{[k_1\cdot(\eta_i p)]^2}}{\varepsilon_1(\eta_i E_p)} = \frac{1}{\Omega}\frac{\sqrt{(k_1\cdot p)^2}}{\varepsilon_1 E_p} \tag{14.29}$$

The cross section for inelastic electron scattering from a point-like quark of type i, carrying four momentum $\eta_i p$ in the $|\mathbf{p}|\to\infty$ frame, in the impulse approximation follows as

$$\begin{aligned} d\sigma^{(i)} &= 2\pi|\bar{T}^{(i)}|^2\delta(W_f-W_i)\frac{\Omega d^3k_2}{(2\pi)^3}\frac{1}{I_0} \\ &= \frac{4\alpha^2}{q^4}\frac{d^3k_2}{2\varepsilon_2}\frac{1}{\sqrt{(k_1\cdot p)^2}}\eta_{\mu\nu}W^{(i)}_{\mu\nu} \end{aligned} \tag{14.30}$$

Here the response tensor for scattering from such a quark is defined by[10]

$$\begin{aligned} W^{(i)}_{\mu\nu} &= -Q_i^2 E_p\sum_{\mathbf{p}'}\frac{1}{2}\sum_{s_1}\sum_{s_2}\bar{u}(p')\gamma_\mu u(\eta_i p)\bar{u}(\eta_i p)\gamma_\nu u(p') \\ &\quad\times\delta_{\mathbf{p}',\eta_i\mathbf{p}-\mathbf{q}}\,\delta(p'_0-\eta_i p_0+q_0) \end{aligned} \tag{14.31}$$

With the use of momentum conservation and the neglect of the masses of the participants, the energy-conserving delta function can be manipulated in the following manner (and this is a key step in the development)

$$\begin{aligned} \delta(p'_0-\eta_i p_0+q_0) &= 2p'_0\,\delta[p'^2_0-(\eta_i p_0-q_0)^2] \\ &= 2p'_0\,\delta[p'^2-(\eta_i p-q)^2] \\ &\approx 2p'_0\,\delta(2\eta_i p\cdot q-q^2) \\ &= \frac{2p'_0}{2p\cdot q}\,\delta(\eta_i-x) \end{aligned} \tag{14.32}$$

Here $x\equiv q^2/2mv$ is the scaling variable introduced in Eq. (14.21). Hence

$$\delta(p'_0-\eta_i p_0+q_0) = \frac{2E_{p'}}{2mv}\delta(\eta_i-x) \tag{14.33}$$

[9] To avoid confusion, we here suppress the subscripts on the S-matrix $S^{(i)}_{fi}$.
[10] This assumes the target is unpolarized; polarization is discussed in the next chapter.

https://doi.org/10.1017/9781009290616.017 Published online by Cambridge University Press

The required traces are the same as those evaluated in $\eta_{\mu\nu}$ at the beginning of this chapter, except that the initial momentum is $\eta_i p$. Thus

$$\begin{aligned} W_{\mu\nu}^{(i)} &= Q_i^2 E_p \frac{2E_{p'}}{2mv}\delta(\eta_i - x)\frac{4}{2E_{p'}2(\eta_i E_p)}\frac{1}{2} \\ &\quad \times \left\{ p'_\mu(\eta_i p_\nu) + (\eta_i p_\mu)p'_\nu - (\eta_i p \cdot p')\delta_{\mu\nu} \right\} \\ &= \frac{Q_i^2}{2mv}\delta(\eta_i - x)\left\{ p'_\mu p_\nu + p'_\nu p_\mu - (p \cdot p')\delta_{\mu\nu} \right\} \end{aligned} \tag{14.34}$$

Now use

$$\begin{aligned} p' &= \eta_i p - q \\ q_\mu \eta_{\mu\nu} &= \eta_{\mu\nu} q_\nu = 0 \end{aligned} \tag{14.35}$$

Hence, again with the neglect of masses,

$$W_{\mu\nu}^{(i)} \doteq \frac{Q_i^2}{2}\delta(\eta_i - x)\left[\delta_{\mu\nu} + \frac{2\eta_i}{mv} p_\mu p_\nu \right] \tag{14.36}$$

The symbol $\doteq$ here indicates that the terms in q_μ and q_ν have been dropped because of Eq. (14.35).

An incoherent sum over all types of quarks with all momentum fractions now gives the response tensor for the composite nucleon

$$W_{\mu\nu} = \sum_{i=1}^{N} \int_0^1 d\eta_i f_i(\eta_i) W_{\mu\nu}^{(i)} \tag{14.37}$$

Substitution of Eq. (14.36) into Eq. (14.37) demonstrates that the response functions now explicitly *exhibit Bjorken scaling* and allows one to identify [see Eqs. (14.37), (14.20), and (14.21)]

$$\begin{aligned} F_1(x) &= \sum_{i=1}^{N} Q_i^2 f_i(x) \\ F_2(x) &= \sum_{i=1}^{N} Q_i^2 x f_i(x) = x F_1(x) \end{aligned} \tag{14.38}$$

Not only do these expressions explicitly exhibit scaling, but they also allow one to calculate the structure functions in terms of the charges of the various types of quarks and their momentum distributions as defined just below Eq. (14.24).

To proceed further, consider the nucleon to be made up of (u, d, s) quarks, with charges listed in Table 14.1, and their antiparticles. It then

https://doi.org/10.1017/9781009290616.017 Published online by Cambridge University Press

Table 14.1. Quark sector used in discussion of deep-inelastic electron scattering from the nucleon.

	u	d	s
Q_i	2/3	−1/3	−1/3

follows from Eq. (14.38) that

$$\begin{aligned}\frac{F_2^p(x)}{x} &= \left(\frac{2}{3}\right)^2[u^p(x)+\bar{u}^p(x)]+\left(\frac{1}{3}\right)^2[d^p(x)+\bar{d}^p(x)] \\ &\quad +\left(\frac{1}{3}\right)^2[s^p(x)+\bar{s}^p(x)] \\ \frac{F_2^n(x)}{x} &= \left(\frac{2}{3}\right)^2[u^n(x)+\bar{u}^n(x)]+\left(\frac{1}{3}\right)^2[d^n(x)+\bar{d}^n(x)] \\ &\quad +\left(\frac{1}{3}\right)^2[s^n(x)+\bar{s}^n(x)] \end{aligned} \tag{14.39}$$

Here an obvious notation has been introduced for the momentum distributions $f_i(x)$ of the various quark types in the proton and neutron.

Strong isospin symmetry implies that the quark distributions should be invariant under the interchange $(d \rightleftharpoons u)$ and hence $(p \rightleftharpoons n)$. Thus one defines

$$\begin{aligned} u^p(x) &= d^n(x) \equiv u(x) \\ d^p(x) &= u^n(x) \equiv d(x) \\ s^p(x) &= s^n(x) \equiv s(x) \end{aligned} \tag{14.40}$$

The quark contributions can be divided into two types: those from *valence* quarks, from which the quantum numbers of the nucleon are constructed; and those from *sea* quarks, present, for example, from $(q\bar{q})$ pairs arising from strong vacuum polarization or mesons in the nucleon.

$$\begin{aligned} u(x) &= u_V(x)+u_S(x) \\ d(x) &= d_V(x)+d_S(x) \\ s(x) &= s_V(x)+s_S(x) \end{aligned} \tag{14.41}$$

Strong vacuum polarization should not distinguish greatly between the types of sea quarks; hence it will be assumed for the purposes of the present arguments that the sea quark distributions are identical

$$S(x) \equiv u_S = \bar{u}_S = d_S = \bar{d}_S = s_S = \bar{s}_S \tag{14.42}$$

https://doi.org/10.1017/9781009290616.017 Published online by Cambridge University Press

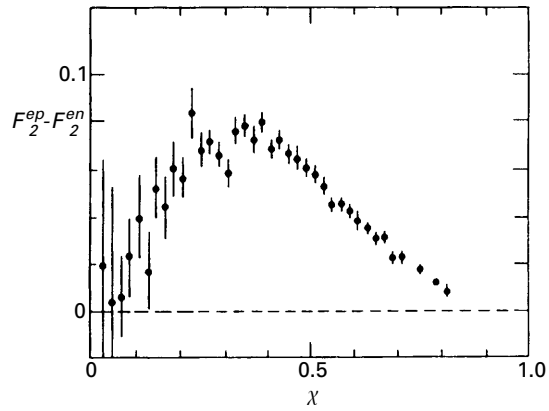

Fig. 14.8. The difference $F_2^p - F_2^n$ as a function of x, as measured in deep-inelastic scattering at the Stanford Linear Accelerator [Ha84].

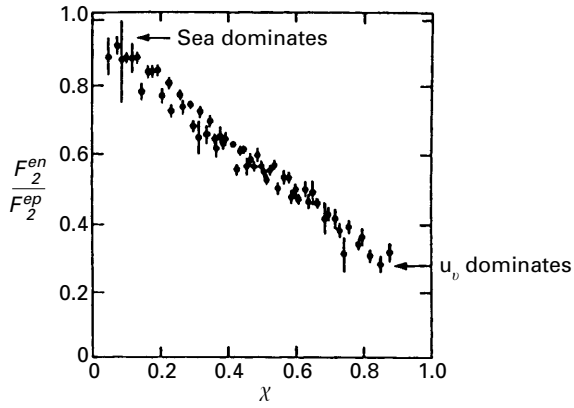

Fig. 14.9. The ratio F_2^n/F_2^p as a function of x, as measured in deep-inelastic scattering. Data are from the Stanford Linear Accelerator [Ha84].

It follows that

$$\begin{aligned} \frac{F_2^p}{x} &= \frac{4}{9}u_V(x) + \frac{1}{9}d_V(x) + \frac{4}{3}S(x) \\ \frac{F_2^n}{x} &= \frac{1}{9}u_V(x) + \frac{4}{9}d_V(x) + \frac{4}{3}S(x) \end{aligned} \tag{14.43}$$

The SLAC data comparing the distribution functions $F_2^{p,n}$ is shown in Figs. 14.8 and 14.9 (taken from [Ha84]). The neutron data were obtained subsequently at SLAC using a ${}^2_1\mathrm{H}$ target. Evidently at small x the ratio $F_2^p/F_2^n \approx 1$ and the sea quark distribution $S(x)$ dominates the structure function; at large x the ratio $F_2^n/F_2^p \approx 0.25$ and it is the valence u quark distribution $u_V(x)$ that dominates.

https://doi.org/10.1017/9781009290616.017 Published online by Cambridge University Press

Consider the momentum sum rule. For simplicity, work in the *nuclear domain* where the nucleon is composed of (u, d) quarks and their anti-quarks. The contribution of these quarks to the momentum sum rule in Eq. (14.27) takes the form

$$\begin{aligned} \zeta_u &\equiv \int_0^1 x\,dx(u+\bar{u}) \\ \zeta_d &\equiv \int_0^1 x\,dx(d+\bar{d}) \end{aligned} \tag{14.44}$$

From the SLAC results [Ha84, Ma90] one finds the sum rules

$$\begin{aligned} \int_0^1 dx F_2^p(x) &= \frac{4}{9}\zeta_u + \frac{1}{9}\zeta_d = 0.18 \\ \int_0^1 dx F_2^n(x) &= \frac{1}{9}\zeta_u + \frac{4}{9}\zeta_d = 0.12 \end{aligned} \tag{14.45}$$

These results, together with Eq. (14.27), then imply

$$\begin{aligned} \zeta_u &= 0.36 \qquad\qquad \zeta_d = 0.18 \\ \zeta_g &= 0.46 \end{aligned} \tag{14.46}$$

Hence one observes that the gluons carry approximately one-half of the momentum of the proton.

We close this section with a very brief discussion of the EMC effect. This material is from [Au83, Mo86, Bi89, Dm90]. The most naive picture of the nucleus is that of a collection of free, non-interacting nucleons. In this picture the structure function one would observe from deep-inelastic electron scattering from a nucleus would be just N times the neutron structure function plus Z times that of the proton. It is an experimental fact, first established by the European Muon Collaboration (EMC), that the quark structure functions are *modified* inside the nucleus [Au83].

It is known that nucleons in the nucleus have a momentum distribution. The most elementary nuclear effect on the structure functions for the nucleus A involves a simple average over the single-nucleon momentum distribution

$$W_{\mu\nu}^{(A)}(P,q) = \sum_{i=1}^{A} \int d^3p |\phi_i(\mathbf{p})|^2 W_{\mu\nu}^{(1)}(p,q) \tag{14.47}$$

We note an immediate difficulty in the extension of the theoretical analysis to an A-body nucleus; this expression is clearly model dependent in the sense that the integration is *not covariant*. It is only with a covariant description of the nuclear many-body system that one can freely transform

https://doi.org/10.1017/9781009290616.017 Published online by Cambridge University Press

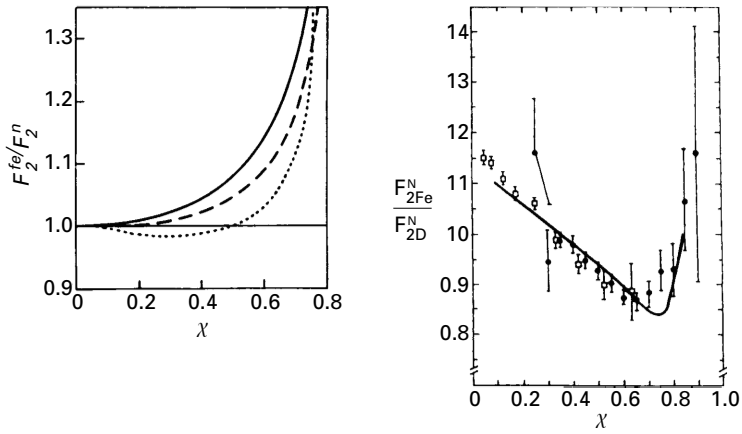

Fig. 14.10. (a) A comparison of calculations of the effect of Fermi smearing on the ratio $\mathscr{R}$ [Bi89]; (b) The ratio $\mathscr{R}$ in a relativistic version of this single-particle model compared with some early experimental data [Mo86].

between Lorentz frames, and, in particular, go to the $|\mathbf{p}| \to \infty$ frame where the parton model is developed.

It will be assumed that Eq. (14.47) holds in the laboratory frame. Define the following ratio

$$\mathscr{R} \equiv \frac{F_2^{\mathrm{Fe}}(x)/A}{F_2^{\mathrm{D}}(x)/2} \tag{14.48}$$

This is the ratio of the structure function for iron (per nucleon) to the structure function for deuterium (per nucleon). Calculations of $\mathscr{R}$ based on Eq. (14.47) are shown in Fig. 14.10(a). $\mathscr{R}$ is calculated assuming the response function $W_{\mu\nu}^{(1)}(p,q)$ for a free nucleon is unmodified in the nuclear interior [Bi89]. Note that this Fermi smearing effect is sizable for large x.

The result of a relativistic version of this single-particle model is shown in Fig. 14.10(b), along with some of the representative early experimental data [Mo86].

https://doi.org/10.1017/9781009290616.017 Published online by Cambridge University Press